Available online at www.sciencedirect.com
SCIENCE DIRECT®
Journal of Chromatography A, 1030 (2004) 3–12
JOURNAL OF CHROMATOGRAPHY A
www.elsevier.com/locate/chroma

Thermodynamics and kinetics of solute transfer in reversed-phase liquid chromatography
Effect of annelation in polycyclic aromatic hydrocarbons

Samuel B. Howerton, Victoria L. McGuffin*

Department of Chemistry, College of Natural Science, Michigan State University, East Lansing, MI 48824-1322, USA

Abstract

A series of four-ring polycyclic aromatic hydrocarbons (PAHs) with varying annelation structure was studied by reversed-phase liquid chromatography. Using a polymeric octadecylsilica stationary phase over a temperature range from 273 to 303 K and an average pressure range from 585 to 3585 psi (1 psi = 6894.76 Pa), the thermodynamic and kinetic aspects of the retention mechanism were examined. Thermodynamic behavior was characterized by the retention factor, together with the associated changes in molar enthalpy and molar volume, whereas kinetic behavior was characterized by the rate constants, together with the associated activation enthalpies and activation volumes. The data indicate that pyrene, with a more condensed annelation structure, exhibits smaller changes in molar enthalpy and molar volume ($\Delta H_{sm} = -4.4$ kcal/mol, $\Delta V_{sm} = -1.9$ ml/mol; 1 cal = 4.184 J) than PAHs with a more linear structure such as chrysene ($\Delta H_{sm} = -8.2$ kcal/mol, $\Delta V_{sm} = -11.7$ ml/mol). The kinetic data indicate that pyrene undergoes faster rates of transport than chrysene ($k_{ms} = 313$ and 14 s^{-1}, respectively), but the non-planar benzo[*c*]phenanthrene undergoes the fastest transport ($k_{ms} = 330\ s^{-1}$). The activation enthalpies and activation volumes are similarly affected by the annelation structure. It is noteworthy that deviations from the exponentially modified Gaussian (EMG) model are observed for some PAH zone profiles at the lowest temperature, which suggests a possible change in retention mechanism. In order to characterize these deviations, the non-linear chromatography (NLC) model and a new bi-exponentially modified Gaussian (E^2MG) model were examined. The regression results indicate that neither the NLC nor E^2MG model offer significant improvements in the statistical quality of fit or provide a better description of the observed retention behavior.

Keywords: Thermodynamic parameters; Kinetic studies; Reversed-phase liquid chromatography; Polynuclear aromatic hydrocarbons

1. Introduction

Reversed-phase liquid chromatography is one of the most common methods for the separation of non-polar solutes. Although many studies have been undertaken to characterize and to validate the retention mechanism, the molecular-level contributions to retention are still not well understood nor fully quantitated. A large number of non-polar solutes have been used to probe reversed-phase systems, one of the more common being the homologous series of alkylbenzenes. These solutes have been used to study the effect of stationary phase alkyl chain length [1,2], mobile-phase composition [1,2], the thermodynamic [3] and kinetic [4] contributions to retention, as well as the differences between silica and zirconia supports [5]. In addition to the alkylbenzenes, other homologues have been used to study phenyl unit addition. The solutes most often employed in these studies are polycyclic aromatic hydrocarbons (PAHs), a class of compounds known to exhibit carcinogenic and mutagenic effects [6–9]. Solutes from this class have included three- to six-ring compounds that are both planar and non-planar. These solutes have been used to study the effect of PAH structure [10–15], stationary phase bonding density [10,12–16], mobile-phase composition [10,16], temperature and pressure [15]. A review by Sander and Wise presents a detailed account of the investigations prior to 1993 [11].

Whereas the effect of ring number has been studied extensively, annelation structure has been the subject of a limited number investigations [16–20]. Four-ring PAH isomers have been used to study the effect of annelation structure with regard to stationary phase bonding density [18,19], mobile-phase composition [17], and temperature [19,20].

* Corresponding author. Tel.: +1-517-355-9715x244; fax: +1-517-353-1793.
E-mail address: jgshabus@aol.com (V.L. McGuffin).

0021-9673/$ – see front matter © 2003 Elsevier B.V. All rights reserved.
doi:10.1016/j.chroma.2003.08.111

Sentell and Dorsey reported that selectivity increases with increasing bonding density [18]. This observation was used to support the theoretical model of Martire and Boehm [21], which suggests that these solutes partition into alkyl-silica bonded phases rather than adsorb. Chmielowiec and Sawatzky reported thermodynamic values for three- and four-ring homologues, which indicate that an increase in length-to-breadth ratio results in more negative changes in molar enthalpy and molar entropy [17]. The more recent investigations by Sentell and Henderson [19], and Sentell et al. [20] have used a homologous series of four-ring PAHs to study the effect of sub-ambient temperature on retention and selectivity. Their data indicate that the selectivity between these solutes increases at lower temperature. This increased selectivity is attributed to the larger surface area for interaction that results from the higher order of the alkyl chains near the proximal terminus, as purported by Stalcup et al. [10]. In addition to four-ring PAHs, six-ring PAHs have also been used as probes of reversed-phase systems. Most notably, phenanthro[3,4-*c*]phenanthrene and tetrabenzonaphthalene have been used to examine the effect of planarity on retention [10–14,16]. However, without the comparison to other six-ring compounds, these non-planar PAHs provide little direct information about the effect of annelation structure.

To date, there have been no systematic studies that consider both the thermodynamic and kinetic behavior as a function of annelation structure. In the present study, a series of four-ring PAHs with planar and non-planar structures are separated on a polymeric octadecylsilica stationary phase with a methanol mobile phase. Using a temperature range from 273 to 303 K and an average pressure range from 585 to 3585 psi (1 psi = 6894.76 Pa), the thermodynamic and kinetic behavior are characterized by previously established methodology [22–24]. The retention factors are calculated, together with the concomitant changes in molar enthalpy and molar volume, to characterize the thermodynamic behavior. The rate constants are calculated, together with the concomitant changes in activation enthalpy and activation volume, to characterize the kinetic behavior. These data provide a holistic view of the effect of annelation structure on the retention mechanism in reversed-phase liquid chromatography.

2. Theory

As previously described [23,24], the calculation of thermodynamic and kinetic contributions to retention requires a synthesis of traditional thermodynamic and transition state theories. The thermodynamic parameters describe the path-independent measures of solute transfer from the mobile to stationary phase. These parameters are calculated from the retention factor (k):

$$k = \frac{t_r - t_0}{t_0} \tag{1}$$

where t_r and t_0 are the elution times of a retained and non-retained solute, respectively. The retention factor is related to the changes in molar enthalpy (ΔH_{sm}) and molar entropy (ΔS_{sm}) by the van't Hoff equation:

$$\ln k = \frac{-\Delta H_{sm}}{RT} + \frac{\Delta S_{sm}}{R} + \ln \beta \tag{2}$$

where R is the universal gas constant and T is the absolute temperature. The molar enthalpy is determined from the slope of a graph of the natural logarithm of the retention factor versus inverse temperature. The change in molar entropy is contained in the intercept, but cannot be reliably quantitated since the phase ratio (β) is a function of both temperature and pressure. From the definition of the molar enthalpy:

$$\ln k = \frac{-\Delta E_{sm} + T\,\Delta S_{sm} - P\,\Delta V_{sm}}{RT} + \ln \beta \tag{3}$$

which is a function of the molar internal energy (ΔE_{sm}) and the pressure–volume work ($P\,\Delta V_{sm}$). The change in molar volume (ΔV_{sm}) is determined from the slope of a graph of the natural logarithm of the retention factor versus pressure (P).

The rate constant for transfer from mobile to stationary phase (k_{sm}) is given by:

$$k_{ms} = \frac{2kt_0}{\tau^2} \tag{4}$$

whereas the rate constant for transfer from stationary to mobile phase (k_{ms}) is given by:

$$k_{sm} = kk_{ms} = \frac{2k^2 t_0}{\tau^2} \tag{5}$$

where τ represents the exponential contribution to variance that arises from slow kinetics [23,24]. During this transfer, the solutes pass through a high-energy transition state (‡) that uniquely characterizes the path-dependent aspects of the retention mechanism. The kinetic rate constants can be used to calculate the activation enthalpies ($\Delta H_{‡m}$, $\Delta H_{‡s}$) and activation volumes ($\Delta V_{‡m}$, $\Delta V_{‡s}$) associated with the transition state via:

$$\ln k_{sm} = \ln A_{‡m} - \frac{\Delta H_{‡m} + RT - P\,\Delta V_{‡m}}{RT} \tag{6}$$

$$\ln k_{ms} = \ln A_{‡s} - \frac{\Delta H_{‡s} + RT - P\,\Delta V_{‡s}}{RT} \tag{7}$$

where $A_{‡m}$ and $A_{‡s}$ are the pre-exponential factors from the Arrhenius equation [23,25,26]. The activation enthalpy can be calculated by graphing the natural logarithm of the rate constant versus inverse temperature at constant pressure. Under the assumption that the activation enthalpy and volume are temperature independent, the activation enthalpy is determined from the slope of the line. Similarly, the activation volume can be calculated from a graph of the natural logarithm of the rate constant versus pressure at constant temperature.

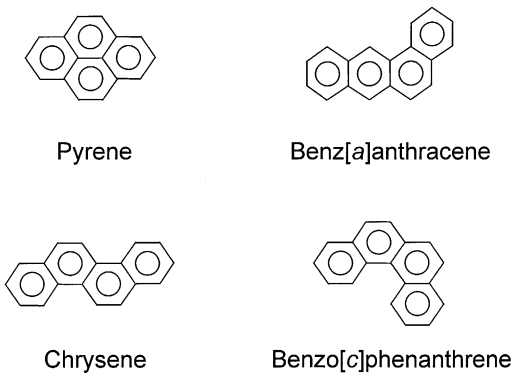

Fig. 1. Structure of the polycyclic aromatic hydrocarbons.

3. Experimental

3.1. Solutes

As depicted in Fig. 1, four polycyclic aromatic hydrocarbons have been chosen to investigate the effect of annelation on the thermodynamics and kinetics of retention. Pyrene, benz[*a*]anthracene, chrysene, and benzo[*c*]phenanthrene (Sigma–Aldrich) were obtained as solids and dissolved in high-purity methanol (Burdick and Jackson, Baxter Healthcare) to yield standard solutions at a concentration of 10^{-4} M. A non-retained marker, 4-methylhydroxy-7-methoxycoumarin [27], was added to each solution at a concentration of 10^{-4} M. To ensure solubility of the PAHs, the solutions were equilibrated at each temperature prior to analysis.

3.2. Experimental system

The PAHs are separated on a capillary liquid chromatography system that has been described previously [15,23,24]. The methanol mobile phase is delivered by a single-piston reciprocating pump (Model 114M, Beckman Instruments), operated in the constant pressure mode. After injection (Model ECI4W1, Valco Instruments), the samples are split between the column and a fused-silica capillary (100 μm i.d., Polymicro Technologies), resulting in an injection volume of 12 nl and a nominal flow rate of 1.30 μl/min. The column is a fused-silica capillary (76 cm × 200 μm i.d., Hewlett-Packard) that is packed via the slurry method and terminated with a quartz wool frit [28]. The silica packing is characterized by a 5.5 μm particle size, 190 Å pore size, and 240 m^2/g surface area (IMPAQ 200, PQ Corp.), reacted with trifunctional octadecylsilane to produce a polymeric phase with bonding density of 5.4 μmol/m^2. A fused-silica capillary (20 μm i.d., Polymicro Technologies) is attached to the column terminus to serve as a restrictor. By reducing the length of the splitter and restrictor proportionally, the pressure drop along the column is held constant as the average pressure is varied from 585 to 3585 psi (±15 psi). The column, injector, splitter, and restrictor are housed within a cryogenic oven (Model 3300, Varian Associates) that enables the temperature to be varied from 273 to 303 K (±0.1 K).

The polyimide coating is removed from the capillary column at two positions (23.2 and 58.3 cm) to facilitate on-column detection by laser-induced fluorescence. The optical and electronic components of this system were designed and constructed in-house to ensure that all contributions to variance are identical at each detection position. A helium–cadmium laser (Model 3074-20M, Melles Griot) provides excitation at 325 nm, which is transmitted to the column by UV-grade optical fibers (100 μm, Polymicro Technologies). The fluorescence signal is collected orthogonal to the incident beam by large diameter optical fibers (500 μm, Polymicro Technologies), isolated by a 420 nm interference filter (S10-410-F, Corion), and detected by a photomultiplier tube (Model R760, Hamamatsu). The resulting photocurrent is amplified, converted to the digital domain (PCI-MIO-16XE-50, National Instruments), and stored by a user-defined program (Labview v5.1, National Instruments).

3.3. Data analysis

After collection, the zone profile for each PAH is extracted from the chromatogram using the previously established conditions for the minimum number of points, integration limits, and signal-to-noise ratio [22]. Each profile is fit by non-linear regression to an appropriate equation, as discussed in the following sections, by using a commercially available program (Peakfit v3.18, SYSTAT Software). The resultant fitting parameters are then subtracted to determine the change between the two detection positions. This method ensures that all measured changes in the solute zone profile arise solely from processes occurring on the column. A result of using this method is that the upper limit of resolution for the rate constants can be expanded beyond that reported in previous work [23].

3.3.1. Exponentially modified Gaussian equation

Under most conditions for this study, the PAH zone profiles are fit to an exponentially modified Gaussian (EMG) equation. The EMG equation is chosen because the statistics of fit are better than for any other model that has been demonstrated to have physical meaning [22,24]. The EMG equation is the convolution of a Gaussian and an exponential function, with the resulting form:

$$C(t) = \frac{A}{2\tau} \exp\left[\frac{\sigma^2}{2\tau^2} + \frac{t_g - t}{\tau}\right]\left[\mathrm{erf}\left(\frac{t - t_g}{\sqrt{2}\sigma} - \frac{\sigma}{\sqrt{2}\tau}\right) + 1\right] \quad (8)$$

where $C(t)$ is the concentration as a function of time, A the peak area, t_g the retention time of the Gaussian component, σ the standard deviation of the Gaussian component, and τ is the exponential component. Symmetrical zone broadening

that arises from processes such as diffusion and mass transfer is quantified by σ. Asymmetrical broadening that arises from volumetric sources (i.e. injectors, unions, etc.), electronic sources (i.e. amplifiers, etc.), and physicochemical processes (i.e. slow kinetics) are quantified by τ. Because asymmetry from volumetric and exponential contributions is constant at each detector, the contribution from slow kinetics can be extracted by difference between the two detectors. The resulting values of the EMG fitting parameters can be used to characterize the thermodynamic and kinetic behavior by means of Eqs. (1), (4) and (5), where:

$$t_r = t_g + \tau \tag{9}$$

In order to ensure that the results from these experiments are statistically reliable, replicate measurements are made at each temperature and pressure. From these replicates, the standard deviations in t_g, τ, and t_0 are used to calculate the propagated error in the retention factor via Eq. (1). The maximum relative error in k is ±0.27%. Similarly, the propagated error in the rate constants is calculated via Eqs. (4) and (5). For both k_{ms} and k_{sm}, the relative error ranges from ±1.9 to 7.1%. The major contribution to the propagated error was found to arise from deviations in τ. The small error in the retention factor and rate constants contributes to the error in the derived quantities such as molar enthalpy, molar volume, activation enthalpy, and activation volume (see below).

At the lowest temperature (273 K), the EMG equation does not show the same quality of fit as at higher temperatures. Hence, two other models are examined to determine whether they provide a better description of the solute zone profiles.

3.3.2. Non-linear chromatography equation

The second model employed to analyze the PAH zone profiles is the non-linear chromatography (NLC) model. Developed initially in 1944 [29], the most current form of the NLC equation was developed by Wade et al. in 1987 [30]:

$$C(t) = \frac{a_0}{a_2 a_3}\left[1 - \exp\left(-\frac{a_3}{a_2}\right)\right] \times \left[\frac{\sqrt{(a_1/x)}I_1(2\sqrt{a_1}x/a_2)\exp((-x-a_1)/a_2)}{1 - T(a_1/a_2, x/a_2)[1-\exp(-a_3/a_2)]}\right] \tag{10}$$

where

$$T(u, v) = e^{-v}\int_0^u e^{-t} I_0(\sqrt{2vt})\, dt \tag{11}$$

and I_0 and I_1 are modified Bessel functions of the first kind. The fitting parameters that are incorporated in the NLC model are the area (a_0), position (a_1), width (a_2), and distortion (a_3). If the chromatographic data are transformed from the time domain to the retention factor domain via Eq. (1), then these parameters can be used to calculate the lumped desorption rate constant:

$$a_2 = \frac{1}{k_{ms} t_0} \tag{12}$$

Using the established relationship between the retention factor and the rate constants ($k = k_{sm}/k_{ms}$), the adsorption rate constant can also be calculated.

3.3.3. Bi-exponentially modified Gaussian equation

Neither the EMG nor NLC equations are capable of evaluating a multiple-site retention model. As a result, a new equation was developed to test whether two distinct sites were present. The bi-exponentially modified Gaussian (E^2MG) equation is the convolution of a Gaussian and two exponential functions, with the resulting form:

$$C(t) = \frac{h\sigma\sqrt{\pi/2}\exp(-(t-t_g)^2/2\sigma^2)}{\tau_1 - \tau_2} \times \left\{\exp\left[\frac{(-t + t_g + (\sigma^2/\tau_1))^2}{2\sigma^2}\right] \times \left[1 + \operatorname{erf}\left(\frac{t\tau_1 - \tau_1 t_g - \sigma^2}{\sqrt{2}\tau_1\sigma}\right)\right] - \exp\left[\frac{(-t + t_g + (\sigma^2/\tau_2))^2}{2\sigma^2}\right] \times \left[1 + \operatorname{erf}\left(\frac{t\tau_2 - \tau_2 t_g - \sigma^2}{\sqrt{2}\tau_2\sigma}\right)\right]\right\} \tag{13}$$

where h is the height, t_g the retention time of the Gaussian component, σ the standard deviation of the Gaussian component, and τ_1 and τ_2 are the exponential components for the first and second kinetic site, respectively. This equation, originally developed by Delley [31], presumes that the two kinetic events are of equal probability.

4. Results and discussion

4.1. Thermodynamic behavior

4.1.1. Retention factors

Representative values of the retention factor are summarized in Table 1. It is apparent that the retention

Table 1
Retention factors for PAH isomers

Solute[a]	k[b]		k[c]	
	273 K	303 K	585 psi	3585 psi
Pyr	1.89	0.84	1.31	1.36
BaA	5.33	1.45	2.99	3.26
Chr	8.12	1.83	4.20	4.64
BcP	1.59	0.80	1.19	1.21

[a] Pyr: pyrene, BaA: benz[*a*]anthracene, Chr: chrysene, BcP: benzo[*c*]phenanthrene.
[b] Retention factor (k) calculated at 3585 psi.
[c] Retention factor (k) calculated at 283 K.

factor for all PAHs decreases with increasing temperature and increases with increasing pressure. Retention also decreases as a function of the length-to-breadth ratio (i.e. pyrene < benz[*a*]anthracene < chrysene), with the exception of benzo[*c*]phenanthrene. As noted previously, benzo[*c*]phenanthrene is slightly non-planar due to steric hindrance of the hydrogen atoms in the bay region. When compared to data reported previously for non-planar six-ring PAHs [23], the retention factor for benzo[*c*]phenanthrene is larger than those for phenanthro[3,4-*c*]phenanthrene and tetrabenzonaphthalene. This suggests that the smaller degree of non-planarity of benzo[*c*]phenanthrene allows for greater interaction with the stationary phase. Moreover, an increase in pressure causes a slight increase in retention for benzo[*c*]phenanthrene, but causes a decrease in retention for phenanthro[3,4-*c*]phenanthrene and tetrabenzonaphthalene. Hence, compression of the stationary phase causes greater interaction of the alkyl chains with benzo[*c*]phenanthrene, similar to the planar solutes, but causes expulsion of the other non-planar solutes.

4.1.2. Molar enthalpy

A representative graph of the logarithm of the retention factor versus the inverse temperature is shown in Fig. 2. The change in molar enthalpy is calculated from the slope of this graph, according to Eq. (2). The graph for each PAH is linear ($R^2 = 0.991$–0.999) and the slope is positive. A positive slope is indicative of a negative change in molar enthalpy and suggests that the transfer from mobile to stationary phase is enthalpically favorable. As shown in Table 2, the most condensed of the planar solutes, pyrene, has the smallest change whereas the least condensed, chrysene, has the greatest change in molar enthalpy. These differences in molar enthalpy can be attributed to the depth that each PAH penetrates into the stationary phase. The proximal regions, where the alkyl group is bound to the silica surface, are highly ordered with all trans carbon–carbon bonds. As the distance from the surface increases, there are more gauche bonds and greater disorder [32–34]. The more condensed PAHs, such as pyrene, probe only the distal regions, whereas less condensed PAHs, such as chrysene, penetrate more deeply into the ordered regions of the stationary phase. Consequently, the change in molar enthalpy becomes more negative the farther the PAH penetrates into the stationary phase. It is noteworthy that benzo[*c*]phenanthrene exhibits changes in molar enthalpy that are smaller than the other PAHs, even though it is not the most condensed. It is hypothesized that the non-planar character of benzo[*c*]phenanthrene does not

Table 2
Molar enthalpy and molar volume for PAH isomers

Solute	ΔH_{sm} (kcal/mol)[a]	ΔV_{sm} (ml/mol)[b]
Pyr	−4.4 ± 0.2	−1.9 ± 1
BaA	−7.1 ± 0.2	−9.6 ± 1
Chr	−8.2 ± 0.2	−11.7 ± 1
BcP	−3.8 ± 0.2	−1.3 ± 1

[a] Molar enthalpy (ΔH_{sm}) calculated at 3585 psi.
[b] Molar volume (ΔV_{sm}) calculated at 283 K.

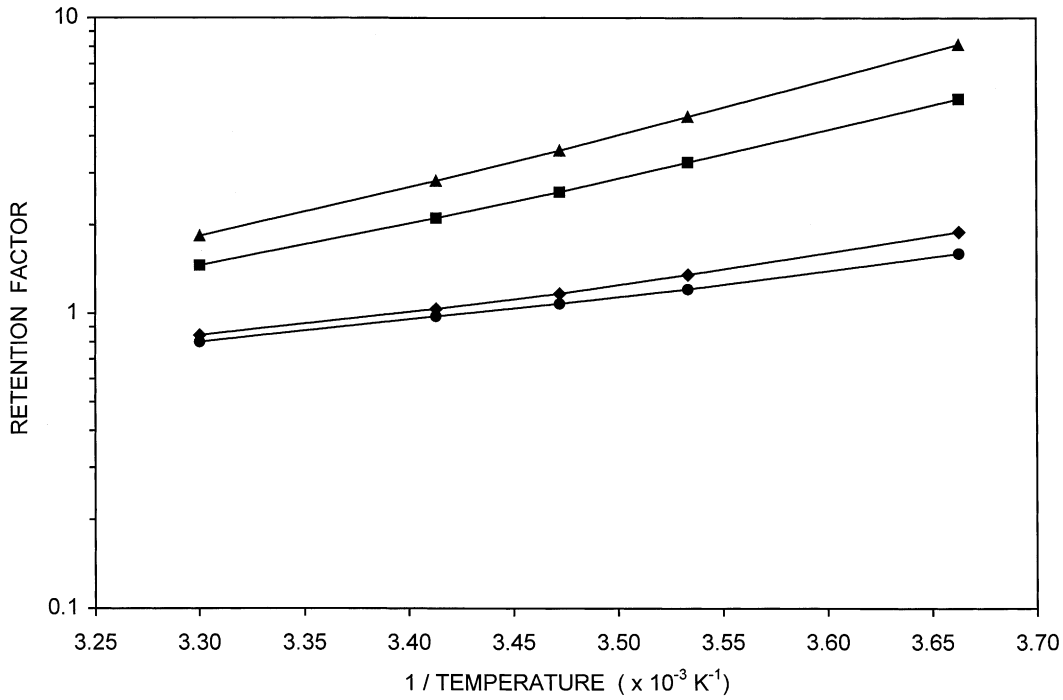

Fig. 2. Representative graph of the retention factor vs. inverse temperature used to calculate the change in molar enthalpy. Column: polymeric octadecylsilica. Mobile phase: methanol, 3585 psi, 0.08 cm/s. Solutes: pyrene (◆), benz[*a*]anthracene (■), chrysene (▲), benzo[*c*]phenanthrene (●). Other experimental details as given in the text.

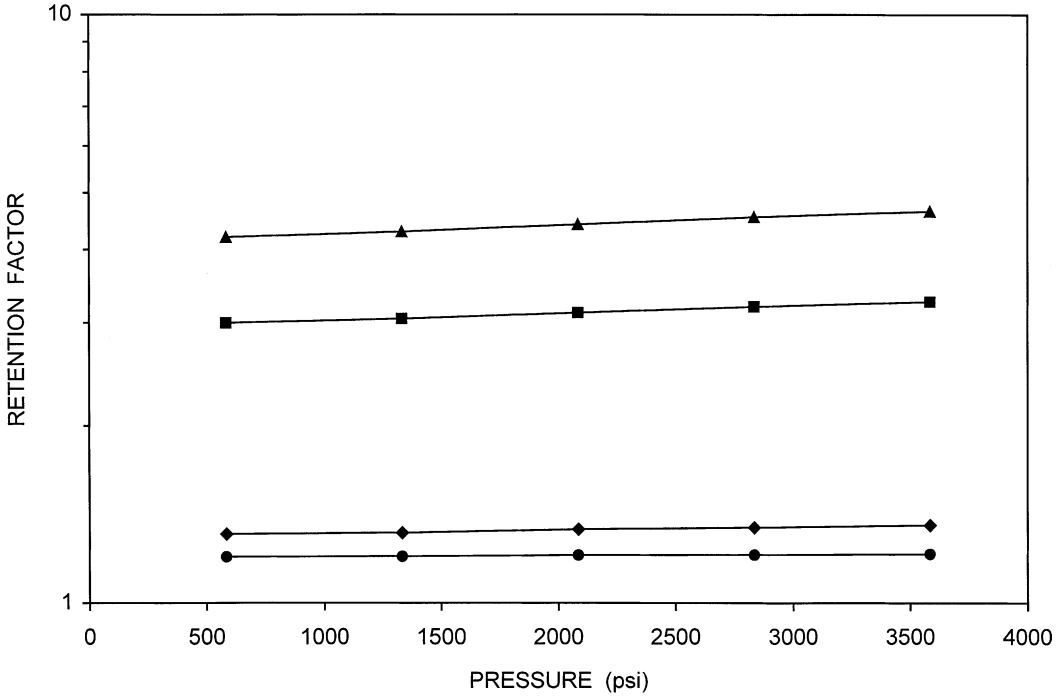

Fig. 3. Representative graph of the retention factor vs. pressure used to calculate the change in molar volume. Column: polymeric octadecylsilica. Mobile phase: methanol, 283 K, 0.08 cm/s. Symbols defined in Fig. 2. Other experimental details as given in the text.

allow it to penetrate as deeply into the high-density polymeric stationary phase. This effect has been noted previously with other non-planar PAHs [11–13,19,20]. The molar enthalpies reported herein are consistent with those in previous investigations [23].

4.1.3. Molar volume

A representative graph of the logarithm of the retention factor versus pressure is shown in Fig. 3. The change in molar volume is calculated from the slope of this graph, according to Eq. (3). Again, the graph for each PAH is linear (R^2 = 0.984–0.998) and the slope is positive. A positive slope is indicative of a negative change in molar volume and suggests that the PAH occupies less volume in the stationary phase than in the mobile phase. As shown in Table 2, the most condensed of the planar solutes, pyrene, has the smallest change whereas the least condensed, chrysene, has the greatest change in molar volume. These differences in molar volume, like the changes in molar enthalpy, can be attributed to the depth that each PAH penetrates into the stationary phase. The more condensed PAHs, such as pyrene, probe only the distal regions, whereas less condensed PAHs, such as chrysene, penetrate more deeply into the ordered regions of the stationary phase. Consequently, the change in molar volume becomes more negative the farther the PAH penetrates into the stationary phase. Again, it is noteworthy that the non-planar solute, benzo[*c*]phenanthrene, has a smaller change in molar volume than the planar solutes. This is consistent with a smaller depth of penetration, as discussed above. However, it is not as extreme as for the six-ring non-planar PAHs, phenanthro[3,4-*c*]phenanthrene and tetrabenzonaphthalene, which exhibit positive changes in molar volume [15,23]. The molar volumes reported herein are consistent with those in previous investigations [23].

4.2. Kinetic behavior

4.2.1. Rate constants

Although the thermodynamic data demonstrate the steady-state aspects of chromatographic behavior, they do not fully explain the retention mechanism. Using the equations and methods developed above, the pseudo-first-order rate constants, activation enthalpies, and activation volumes were calculated. These values help to quantify the kinetic aspects of PAH transfer between the mobile and stationary phases as a function of the annelation structure.

Representative values of the rate constants, calculated using Eqs. (4) and (5), are summarized in Tables 3 and 4. The most condensed of the planar solutes, pyrene, has the largest rate constants, whereas the least condensed, chrysene, has the smallest rate constants for transport from mobile to stationary phase (k_{sm}) and from stationary to mobile phase (k_{ms}). However, the non-planar solute, benzo[*c*]phenanthrene, has larger rate constants than the planar solutes. As shown in Table 3, the rate constants for all PAHs increase with increasing temperature. This behavior is a consequence of the increased diffusion coefficients and the enhanced fluidity of the stationary phase. As more kinetic energy is imparted, the alkyl chains become more labile and can more readily undergo rotation of the

Table 3
Rate constants for PAH isomers calculated by using the exponentially modified Gaussian (EMG) model as a function of temperature[a]

Solute	k_{ms} (s^{-1})		k_{sm} (s^{-1})	
	283 K	293 K	283 K	293 K
Pyr	198	1137	269	1179
BaA	74	521	241	1099
Chr	7	58	34	163
BcP	216	1360	262	1330

[a] Rate constants from stationary to mobile phase (k_{ms}) and from mobile to stationary phase (k_{sm}) calculated at 3585 psi.

Table 4
Rate constants for PAH isomers calculated by using the exponentially modified Gaussian (EMG) model as a function of pressure[a]

Solute	k_{ms} (s^{-1})		k_{sm} (s^{-1})	
	585 psi	3585 psi	585 psi	3585 psi
Pyr	313	198	411	269
BaA	73	62	224	202
Chr	14	7	61	34
BcP	330	216	395	262

[a] Rate constants from stationary to mobile phase (k_{ms}) and from mobile to stationary phase (k_{sm}) calculated at 283 K.

carbon−carbon bonds from the trans to gauche conformation. In fact, this polymeric octadecylsilica stationary phase is known to undergo a phase transition in the vicinity of 318 K [15,24]. This increased lability enables the PAHs to diffuse in and out of the stationary phase more freely. As shown in Table 4, the rate constants for all PAHs decrease with increasing pressure. This behavior is a consequence of the compression of the alkyl chains, which impedes the PAH diffusion in and out of the stationary phase.

4.2.2. Activation enthalpy

A representative graph of the logarithm of the rate constant versus the inverse temperature is shown in Fig. 4. The activation enthalpy is calculated from the slope of this graph, according to Eqs. (6) and (7). As shown in Table 5, there are slight differences that indicate the most condensed solute, pyrene, has the smallest activation enthalpies whereas the least condensed solute, chrysene, has the greatest activation enthalpy. However, given the uncertainties in these values, the differences are not statistically significant. The similarity in values implies that the activation enthalpy is largely independent of annelation structure, and suggests that the PAHs encounter a similar barrier at the interface between the mobile and stationary phases. As the activation enthalpy are compared to one another and to the change in molar enthalpy in Table 2, a trend emerges: $\Delta H_{\ddagger s} > \Delta H_{\ddagger m} \gg \Delta H_{sm}$. Thus, the enthalpic barrier for the transition is significantly greater than the thermodynamic change in molar enthalpy.

4.2.3. Activation volume

A representative graph of the natural logarithm of the rate constant versus pressure is shown in Fig. 5. The activation volume is calculated from the slope of this graph, according to Eqs. (6) and (7). In contrast to the activation enthalpies, the activation volumes are a statistically significant function of the annelation structure. As shown in Table 6, the most

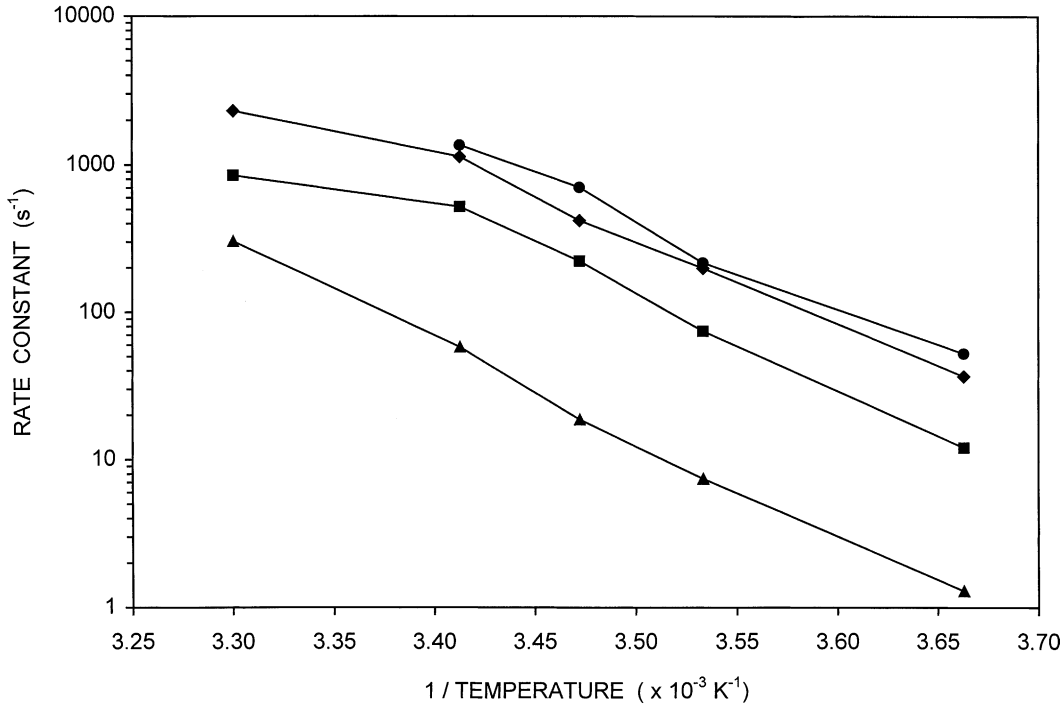

Fig. 4. Representative graph of the rate constant (k_{ms}) vs. inverse temperature used to calculate the activation enthalpy. Column: polymeric octadecylsilica. Mobile phase: methanol, 3585 psi, 0.08 cm/s. Symbols defined in Fig. 2. Other experimental details as given in the text.

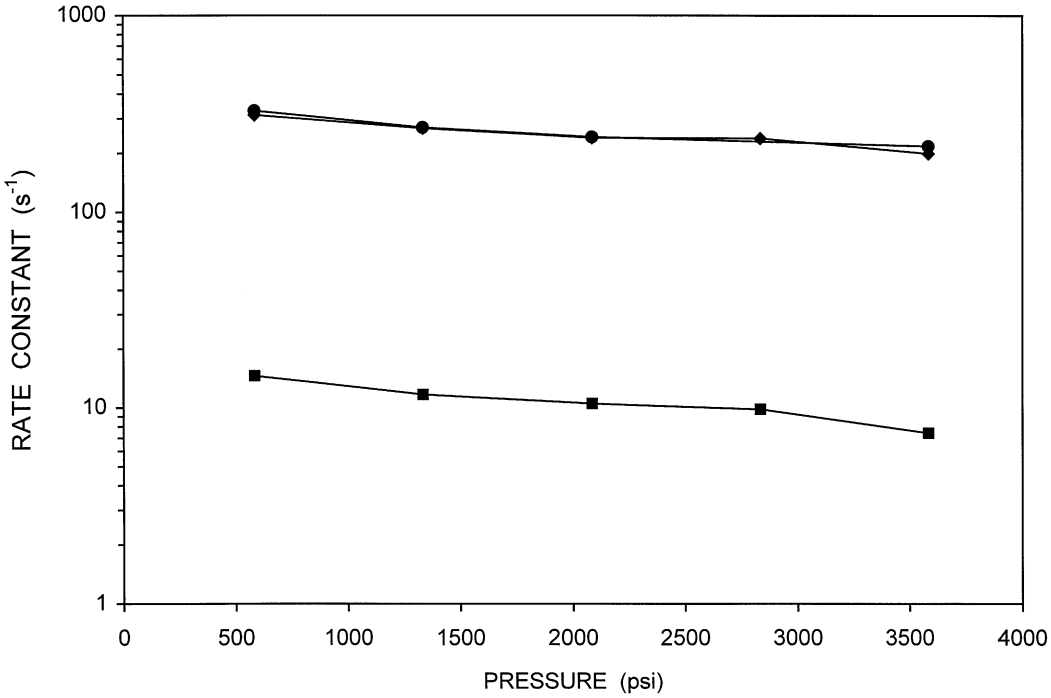

Fig. 5. Representative graph of the rate constant (k_{ms}) vs. pressure used to calculate the activation volume. Column: polymeric octadecylsilica. Mobile phase: methanol, 283 K, 0.08 cm/s. Symbols defined in Fig. 2. Other experimental details as given in the text.

condensed of the planar solutes, pyrene, has the smallest activation volume whereas the least condensed, chrysene, has the greatest activation volume. The non-planar solute, benzo[*c*]phenanthrene has a smaller activation volume than the planar solutes. Similar to the enthalpic trends, the activation volumes and the change in molar volume demonstrate the trend of $\Delta V_{\ddagger s} > \Delta V_{\ddagger m} \gg \Delta V_{sm}$. Hence, the volumetric barrier for the transition is large, even though the overall change in molar volume is relatively small.

4.2.4. Kinetic deviations

In the studies presented above, the PAH zone profiles were fit very well by the EMG equation, with typical R^2 values of 0.99 or greater. However, it was noted that the quality of fit was degraded slightly for some PAHs at the lowest temperature (273 K), with R^2 values of 0.98–0.99 and small non-random residuals along the tailing edge of the zone profile. As these deviations from the EMG model may potentially arise from a change in the retention mechanism, more detailed investigation was warranted. First, in order to ensure that this effect did not arise from limited solubility, the PAH solutions were equilibrated at 273 K prior to injection. No statistically significant differences were observed in the PAH zone profiles or the quality of fit to the EMG equation.

To examine whether the low temperature causes a change in the retention mechanism, two alternative models were examined. The first alternative was the non-linear chromatography model. The retention factors for the PAHs increase with decreasing temperature (Table 1), thereby increasing the concentration in the stationary phase. Hence, the isotherm might be expected to deviate from linearity at low temperature. Accordingly, the NLC model (Eq. (10)) was used to iteratively fit each of the PAH zone profiles that showed deviant behavior. This model, too, gave R^2 values of 0.98–0.99 and exhibited small non-random residuals from the observed zone profiles. As shown in Table 7, the quality of fit for the NLC and EMG models was

Table 5
Activation enthalpies for PAH isomers[a]

Solute	$\Delta H_{\ddagger s}$ (kcal/mol)	$\Delta H_{\ddagger m}$ (kcal/mol)
Pyr	24 ± 3	19 ± 3
BaA	25 ± 4	17 ± 3
Chr	31 ± 2	23 ± 2
BcP	27 ± 3	23 ± 3

[a] Activation enthalpies from stationary phase to transition state ($\Delta H_{\ddagger s}$) and from mobile phase to transition state ($\Delta H_{\ddagger m}$) calculated at 283 K and 3585 psi.

Table 6
Activation volumes for PAH isomers[a]

Solute	$\Delta V_{\ddagger s}$ (ml/mol)	$\Delta V_{\ddagger m}$ (ml/mol)
Pyr	47 ± 7	43 ± 7
BaA	NR[b]	NR
Chr	69 ± 9	57 ± 9
BcP	38 ± 13	37 ± 13

[a] Activation volumes from stationary phase to transition state ($\Delta V_{\ddagger s}$) and from mobile phase to transition state ($\Delta V_{\ddagger m}$) calculated at 283 K.

[b] Not statistically reliable (NR) owing to large relative standard deviation (>100% R.S.D.).

Table 7
Rate constants for PAH isomers calculated by using the exponentially modified Gaussian (EMG) and non-linear chromatography (NLC) models[a]

Solute	EMG			NLC		
	k_{ms} (s^{-1})	k_{sm} (s^{-1})	R^2 [b]	k_{ms} (s^{-1})	k_{sm} (s^{-1})	R^2 [b]
Pyr	38	69	0.996	12	23	0.999
BaA	12	64	0.994	7	37	0.999
Chr	1	11	0.987	6	44	0.993
BcP	52	84	0.997	12	20	0.999

[a] Rate constants from stationary to mobile phase (k_{ms}) and from mobile to stationary phase (k_{sm}) calculated at 273 K and 3585 psi.
[b] Square of correlation coefficient for non-linear regression (R^2).

similar. The rate constants are of the same order of magnitude, but those determined by the NLC model are somewhat smaller than those determined by the EMG model for pyrene, benz[*a*]anthracene, and benzo[*c*]phenanthrene but somewhat larger for chrysene.

As neither the EMG nor NLC model described the data well, a third model, the bi-exponentially modified Gaussian equation, was examined. This model is appropriate if there are two sites in the stationary phase with significantly different kinetic behavior. This behavior may arise from two partition sites or partition and adsorption sites. Accordingly, the E^2MG model (Eq. (13)) was used to iteratively fit each of the PAH zone profiles that showed deviant behavior. These results, summarized in Table 8, indicate that this equation also had difficulty in fitting the zone profiles. For chrysene, the regression failed owing to overflow and underflow errors. For the other PAHs, the E^2MG equation forces τ_1 and τ_2 to assume values very close to one another. The rate constants are the same for both sites, but are larger than those calculated using either the EMG or NLC models. These values imply that the kinetic sites are equally distributed and the same in their energetic natures.

It is evident from Tables 7 and 8 that neither the NLC nor the E^2MG model provides a more accurate description of the solute zone profiles than the EMG model. The origin of the unusual zone profiles that lead to poor fitting with these models is under further investigation.

Table 8
Rate constants for PAH isomers calculated by using the bi-exponentially modified Gaussian (E^2MG) model for two sites[a]

Solute	Site 1		Site 2		R^2 [b]
	k_{ms} (s^{-1})	k_{sm} (s^{-1})	k_{ms} (s^{-1})	k_{sm} (s^{-1})	
Pyr	79	148	79	148	0.999
BaA	32	171	32	171	0.998
Chr	NR[c]	NR	NR	NR	–
BcP	24	37	24	37	0.998

[a] Rate constants from stationary to mobile phase (k_{ms}) and from mobile to stationary phase (k_{sm}) calculated at 273 K and 3585 psi.
[b] Square of correlation coefficient for non-linear regression (R^2).
[c] Not statistically reliable (NR) owing to overflow and underflow errors in non-linear regression.

5. Summary

In this study, the thermodynamic and kinetic behavior of four-ring PAHs was examined in reversed-phase liquid chromatography. Even though the changes in molar enthalpy and molar volume are relatively small, the kinetic data suggest that the barrier for transition between mobile and stationary phases is large. For a solute like chrysene, the activation enthalpy is 23 kcal/mol (1 cal = 4.184 J) for entry into the stationary phase, and 31 kcal/mol for exit from the stationary phase. There is a similarly large activation volume for each transition (69 and 57 ml/mol, respectively). These relatively large values for activation enthalpy and activation volume suggest that the transition is more likely to occur in a series of discrete steps rather than in a single step. When the values for chrysene are compared to those for pyrene, it is apparent that the annelation structure influences the energy and volume contributions to the retention mechanism.

In addition, the anomalous behavior at 273 K suggests that the retention mechanism may not be static for these molecules. It is important to emphasize that this behavior is not apparent from the thermodynamic (steady state) measurements. The kinetic measurements are essential to make inferences about the mechanism. It is also important that these measurements be derived concurrently from the same data, so that the thermodynamic and kinetic measurements are internally consistent. From the examined models, there is no conclusive evidence for a non-linear isotherm or for multiple sites with different kinetic behavior. This anomalous behavior at sub-ambient temperatures warrants further investigation, as it may contribute to the changes in selectivity reported in previous investigations [17,19].

Acknowledgements

The authors gratefully acknowledge Dr. Lane C. Sander (National Institute of Standards and Technology) for synthesis of the polymeric octadecylsilica stationary phase. In addition, the assistance of Drs. Peter E. Krouskop and Peiru Wu (Michigan State University) in the convolution of the E^2MG function is appreciated. S.B.H. acknowledges support through the James. L. Dye Fellowship from the Department of Chemistry, as well as the Dr. Marvin Hensley Fellowship from the College of Natural Science at Michigan State University.

References

[1] A. Tchapla, H. Colin, G. Guiochon, Anal. Chem. 56 (1984) 621.
[2] J. Ko, J. Chilenski, T. Rodgers, J.C. Ford, J. Chromatogr. A 913 (2001) 15.
[3] R.P.J. Ranatunga, P.W. Carr, Anal. Chem. 72 (2000) 5679.
[4] K. Miyabe, S. Sotoura, G. Guiochon, J. Chromatogr. A 919 (2001) 231.
[5] J. Zhao, P.W. Carr, Anal. Chem. 72 (2000) 302.

[6] M. Cooke, A.J. Dennis, G.L. Fisher, Polynuclear Aromatic Hydrocarbons: Physical and Biological Chemistry, Battelle Press, Columbus, OH, 1982.
[7] M.R. Osborne, N.T. Crosby, Benzopyrenes, Cambridge University Press, New York, 1987.
[8] T. Vo-Dinh, Chemical Analysis of Polycyclic Aromatic Hydrocarbons, Wiley, New York, 1988.
[9] R.F. Hertel, G. Rosner, J. Kielhorn, Selected Non-Heterocyclic Polycyclic Aromatic Hydrocarbons, World Health Organization, Geneva, 1998.
[10] A.M. Stalcup, D.E. Martire, S.A. Wise, J. Chromatogr. 442 (1988) 1.
[11] L.C. Sander, S.A. Wise, J. Chromatogr. A 656 (1993) 335.
[12] L.C. Sander, M. Pursch, S.A. Wise, Anal. Chem. 71 (1999) 4821.
[13] L.C. Sander, S.A. Wise, Anal. Chem. 67 (1995) 3284.
[14] J. Wegmann, K. Albert, M. Pursch, L.C. Sander, Anal. Chem. 73 (2001) 1814.
[15] V.L. McGuffin, S.H. Chen, J. Chromatogr. A 762 (1997) 35.
[16] S.R. Cole, J.G. Dorsey, J. Chromatogr. 635 (1993) 177.
[17] J. Chmielowiec, H. Sawatzky, J. Chromatogr. Sci. 17 (1979) 245.
[18] K.B. Sentell, J.G. Dorsey, J. Chromatogr. 461 (1989) 193.
[19] K.B. Sentell, A.N. Henderson, Anal. Chim. Acta 246 (1991) 139.
[20] K.B. Sentell, N.I. Ryan, A.N. Henderson, Anal. Chim. Acta 307 (1995) 203.
[21] D.E. Martire, R.E. Boehm, J. Phys. Chem. 87 (1983) 1045.
[22] S.B. Howerton, C. Lee, V.L. McGuffin, Anal. Chim. Acta 478 (2003) 99.
[23] S.B. Howerton, V.L. McGuffin, Anal. Chem. 75 (2003) 3539.
[24] V.L. McGuffin, C. Lee, J. Chromatogr. A 987 (2003) 3.
[25] K.J. Laidler, Chemical Kinetics, third ed., Harper & Row, New York, 1987.
[26] J.I. Steinfeld, J.S. Francisco, W.L. Hase, Chemical Kinetics and Dynamics, second ed., Prentice Hall, Upper Saddle River, NJ, 1999.
[27] V.L. McGuffin, S.H. Chen, Anal. Chem. 69 (1997) 930.
[28] J.C. Gluckman, A. Hirose, V.L. McGuffin, M. Novotny, Chromatographia 17 (1983) 303.
[29] H.C. Thomas, J. Am. Chem. Soc. 66 (1944) 1664.
[30] J.L. Wade, A.F. Bergold, P.W. Carr, Anal. Chem. 59 (1987) 1286.
[31] R. Delley, Anal. Chem. 58 (1986) 2344.
[32] C.J. Orendorff, M.W. Ducey Jr., J.E. Pemberton, J. Phys. Chem. A 106 (2002) 6991.
[33] M.W. Ducey Jr., C.J. Orendorff, J.E. Pemberton, L.C. Sander, Anal. Chem. 74 (2002) 5576.
[34] M.W. Ducey Jr., C.J. Orendorff, J.E. Pemberton, L.C. Sander, Anal. Chem. 74 (2002) 5585.